

RESEARCH

Open Access



# Identification of common stria vascularis cellular alteration in sensorineural hearing loss based on ScRNA-seq

Xi Gu<sup>2,3,4†</sup>, Kanglun Jiang<sup>5†</sup>, Ruru Chen<sup>1†</sup>, Zhifeng Chen<sup>2,3,4†</sup>, Xianmin Wu<sup>6†</sup>, Haijie Xiang<sup>1</sup>, Xinsheng Huang<sup>5\*</sup> and Benyu Nan<sup>1\*</sup>

## Abstract

**Background** The stria vascularis (SV), located in the lateral wall of the cochlea, maintains cochlear fluid homeostasis and mechano-electrical transduction (MET) activity required for sound wave conduction. The pathogenesis of a number of human inheritable deafness syndromes, age related hearing loss, drug-induced ototoxicity and noise-induced hearing loss results from the morphological changes and functional impairments in the development of the SV. In this study, we investigate the implications of intercellular communication within the SV in the pathogenesis of sensorineural hearing loss (SNHL). We aim to identify commonly regulated signaling pathways using publicly available single-cell transcriptomic sequencing (scRNA-seq) datasets.

**Methods** We analyzed scRNA-seq data, which was derived from studying the cochlear SV in mice with SNHL compared to normal adult mice. After quality control and filtering, we obtained the major cellular components of the mouse cochlear SV and integrated the data. Using Seurat's FindAllMarkers and FindMarkers packages, we searched for novel conservative genes and differential genes. We employed KEGG and GSEA to identify molecular pathways that are commonly altered among different types of SNHL. We utilized pySCENIC to discover new specific regulatory factors in SV subpopulation cells. With the help of CellChat, we identified changes in subpopulation cells showing similar trends across different SNHL types and their alterations in intercellular communication pathways.

**Results** Through the analysis of the integrated data, we discovered new conserved genes to SV specific cells and identified common downregulated pathways in three types of SNHL. The enriched genes for these pathways showing similar trends are primarily associated with the Electron Transport Chain, related to mitochondrial energy metabolism. Using the CellChat package, we further found that there are shared pathways in the incoming signaling of specific intermediate cells in SNHL, and these pathways have common upstream regulatory transcription factor of Nfe2l2. Combining the results from pySCENIC and CellChat, we predicted the transcription factor Nfe2l2 as an upstream regulatory factor for multiple shared cellular pathways in IC. Additionally, it serves as an upstream factor for several genes within the Electron Transport Chain.

<sup>†</sup>Xi Gu, Kanglun Jiang, Ruru Chen, Zhifeng Chen, and Xianmin Wu contributed equally to this work.

\*Correspondence:

Xinsheng Huang  
huang.xinsheng@zs-hospital.sh.cn

Benyu Nan  
benyu2003@icloud.com

Full list of author information is available at the end of the article



**Conclusion** Our bioinformatics analysis has revealed that downregulation of the mitochondrial electron transport chain have been observed in various conditions of SNHL. E2f1, Esrrb, Runx1, Yy1, and Gata2 could serve as novel important common TFs regulating the electron transport chain. Adm has emerged as a potential new marker gene for intermediate cells, while Itgb5 and Tesc show promise as potential new marker genes for marginal cells in the SV. These findings offer a new perspective on SV lesions in SNHL and provide additional theoretical evidence for the same drug treatment and prevention of different pathologies of SNHL.

**Keywords** Sensorineural hearing loss (SNHL), Stria vascularis, ScRNA-seq, Transcription factors (TF), Cell–cell communication

## Introduction

To a large extent, hearing sensitivity depends on the fine structure of the cochlea and its ability to convert sound waves into encoded impulses in the auditory nerve [1]. The conversion in the cochlea is performed by mechano-electrical transduction (MET) channels in hair bundles of hair cells [2]. To maintain MET activity, the stria vascularis (SV), located in the inner side of the lateral wall, produces a high level of cochlear endopotential (+80 mV) and a high potassium concentration (~150 mM) for the scala media [3, 4]. The morphological changes and functional impairments in the development of SV are involved in multiple human inheritable deafness syndromes, age-related hearing loss (ARHL), drug-induced ototoxicity and noise-related hearing loss (NRHL) [5–7].

Extensive experimental research has shown that high cisplatin accumulation and distribution in the SV were found both in human and mouse cochlear tissue [8]. Cisplatin ototoxicity is mainly manifested by SV damage in the basal turn: edema, swelling, rupture and compression of marginal cells (MC), and depletion of organelles in cells [9]. Subsequent shrinkage in the SV area could be detected after more than four weeks of recovery from cisplatin administration, and the diminishment was caused mostly by a decrease in the areas of the intermediate and marginal cells [7]. However, we currently have a limited understanding of the cellular and molecular mechanisms of SV injury in cisplatin-related hearing loss (CRHL).

In modern society, more than 12% of the global population suffers from NRHL attributed to ever-increasing levels of noise exposure [10]. Many researchers found that noise exposure in animals could result from decreasing vessel diameter and increasing microvascular permeability and macromolecular transport in the cochlear SV [11–13]. Mouse experiments indicate that noise exposure leads to MC and blood vessel morphological changes, inducing dysfunction of cochlear microcirculation [14].

Age-related hearing loss (ARHL) is a complex hearing impairment that occurs as a natural part of aging and is one of the most common health conditions affecting

the elderly following heart disease and arthritis [15]. It affects a significant portion of the aging population and is characterized by a gradual decline in the ability to hear high-frequency sounds. Approximately one-third of the population aged 65 and 74 has some degree of hearing impairment, and the number of people over the age of 75 has increased to roughly half. The exact pathology of ARHL is not fully detected and is likely to involve a combination of aging, genetics, and environmental factors, such as exposure to loud noise. Alterations in the SV play a pivotal role in the pathogenesis of ARHL and can contribute to the decline in hearing associated with this condition [16].

The three main causes of sensorineural hearing loss (SNHL), aging, noise and cisplatin exposure, have great similarities in the pathophysiological degeneration of the cochlea. To date, many molecular mechanisms have been suggested to be responsible for these similarities, but systematic validation is still lacking. Bulk data from three models showed that gene coexpression in inflammation, immunity, apoptosis and ion transport significantly correlated with each other in the hair cells of the cochlea [17, 18]. Increasing inflammatory factors IL1B and CCL2 inducing ROS-related apoptosis in the whole cochleae of SNHL were identified by previous studies *in vitro* and *in vivo* [19].

Many studies have shown that CRHL and NRHL share some common processes in the cochlea, such as inflammation and oxidative stress, but the changes in response to cisplatin and noise are extremely different. Prior to the advent of single-cell RNA-seq (scRNA-seq), research on SNHL focused on the entire cochlea and hair cells, lacking systematic studies on the cochlear SV. To further explore the SV pathology in SNHL, we gathered and compared datasets derived from scRNA-seq to identify and filter out conservative gene markers and common pathways related to aging, cisplatin exposure, and noise response in the cochlear SV. This analysis aimed to uncover potential targets and provide more evidence for broadly effective therapeutic agents in the treatment of SNHL.

## Materials and methods

### Online Published scRNA-seq Data Collection and Processing

Collecting scRNA-seq data of the cochlear SV from the Gene Expression Omnibus (GEO) repository and the Genome Sequence Archive in National Genomics Data Center (NGDC), CRA004814, GSE165662, and GSE168041 were used for analysis of different treatment models in SNHL. The details and mouse cell information of the datasets in the GEO and NGDC are listed in Table 1.

We obtained cochlear stria vascularis samples from four groups of mice exposed to various treatment protocols. In the CIHL group, mice received an intraperitoneal (IP) injection of 14 mg/kg cisplatin 24 h before euthanasia ( $n=6$ , three females, three males). The NIHL group was exposed to a two-hour duration of octave band noise centered at 11.3 kHz (8-16 kHz) with a sound pressure level (SPL) of 105 dB ( $n=4$ ). The samples for scRNA-seq of 1- and 15-month-old groups contain 5 males and 5 females.

The Cell Ranger (7.1.0) pipeline developed by 10×Genomics was applied to analyze the aged SV cells downloaded from NDGC (CRA004814) in fastq format, which were then aligned (the mouse reference genome-mm10), filtered, and quantified. The final output is a matrix of gene expression levels for each individual cell in the experiment, allowing for further analysis using tools such as dimensionality reduction, clustering, and differential expression analysis. The Seurat 4.3.0 library in R 4.2.0 was applied to analyze the single-cell transcriptome.

The R package *sctransform* (Hafemeister and Satija, 2019), which included the selection of variable genes, was applied to normalize the datasets. We performed principal component analysis (PCA) to reduce dimensionality on the normalized data matrix using the top 2000 most highly variable genes. For 2D visualization, PC embeddings were passed into Uniform Manifold Approximation and Projection (UMAP) [20]. Marker genes of the clusters were explored using the Seurat *FindAllMarkers* function (Wilcoxon rank-sum test,  $\text{min.pct}=0.25$ ,  $\text{log-change threshold}=0.25$ ). The clusters in the datasets were annotated based on established markers. We employed Harmony to integrate SV major cells from datasets with different SNHL. Differentially expressed genes (DEGs) of the clusters integrated by harmony between various SNHL were explored by the Seurat *FindMarkers* function.

### Kyoto Encyclopedia of Genes and Genomes (KEGG) and Gene Set Enrichment Analysis (GSEA) application in functional enrichment

The common conserved genes in different clusters from different SNHL were clustered and analyzed by KEGG. GSEA-WikiPathway analyses were conducted on WebGestalt 2019 (<https://www.webgestalt.org/>) to detect different molecular mechanisms and underlying pathways comparing the aged, cisplatin-treated, and noise-treated groups with the adult group. The normalized enrichment score was obtained by gene set permutations 1,000 times, and an FDR value of 0.05 was set to filter the significant enrichment results.

**Table 1** List of details and mouse information of the datasets

ID	Single Cell Types	Mouse Model	Mouse Age	Treatments	Mouse Strain	Platforms	Cells Number Included
CRA004814	Stria Vascularis	Adult Mouse	P30	No	C57BL/6 J	Illumina NovaSeq 6000	1390
GSE165662	Stria Vascularis	Cisplatin-treated Adult Mouse	P30	intraperitoneal (IP) injection of 14 mg/kg cisplatin 24 h prior to sacrifice	CBA/J	No	1242
GSE168041	Stria Vascularis	Noise-exposed Adult Mouse	2 to 4 months old	Noise trauma was induced with an octave band of noise centered at 11.3 kHz (8-16 kHz) at 105 dB sound pressure level (SPL) for 2 h and were euthanized in 6 h or 24 h post-noise exposure	CBA/CaJ	Illumina NovaSeq 6000	5913
CRA004814	Stria Vascularis	Senior Mouse	15 months old	No	C57BL/6 J	Illumina NovaSeq 6000	2149

### Inference of gene regulatory network by pySCENIC

We extract counts from the integrated data, convert it into CSV format, and then read it into Python and output it as a Loom format file. A three-step pipeline is applied to output the Loom format file. First, transcription factors (TFs) combined with their target genes to define a regulon are derived using gene inference (RcisTarget mm9 motif databases) methods that are entirely correlated between the expression of genes across cells. Then, based on the presence of cis-regulatory footprints, these regulons are refined effectively to separate direct from indirect targets. Finally, the original cells are differentiated and clustered according to the activity of these discovered regulons. The pySCENIC output in the form of a loom file was subsequently analyzed utilizing the SCoPeLoomR R package. The activity of each regulon was evaluated in the scoring step using AUCcell. For visualization purposes, we generated a binary heatmap using the output area under the recovery curve (AUC) values and AUC thresholds. This allowed us to determine the validity of a particular rule within a given cell.

In addition to plotting the binary values, we also transformed these AUC values into a range from 0 to 1 for each regulon and represented them in a heatmap with a color scale. The pheatmap package was used to generate the heatmap and perform hierarchical clustering of the regulons.

### CellChat

The CellChat package includes a comprehensive signaling molecule interaction database, which can infer cellular communication and provide functional data exploration, analysis and visualization. By using CellChat, we were able to infer cell–cell interactions among different subsets of SV [21]. Based on a permutation test, we calculated the most enriched ligand–receptor interactions. *P* values less than 0.01 were considered significant. First, we extracted single-cell data from the integrated Seurat dataset for different treatment groups and created a CellChat object. Then, we combined the CellChat objects for the different treatment groups and performed the following three-step data process on the merged data: 1. Predict general principles of cell–cell communication in different treatments; 2. Identify the conserved and context-specific signaling pathways; 3. Identify the upregulated and downregulated signaling ligand–receptor pairs between specific cells in different treatments. Finally, we visualized the cell–cell communication network using a hierarchy plot, circle plot or chord diagram.

## Results

### Cell type identification

First, a total of three published scRNA-seq datasets of mouse SV were obtained from GEO and NGDC. After quality control and preprocessing of the data to remove low-quality cells, performing normalization and eliminating batch effects, single cells dissociated from mouse SV of different treatments were clustered into three major clusters. Classic known cell-specific genes described in previous studies were used to annotate cell clusters: intermediate cells (IC, *Kcnj10*<sup>+</sup>, *Kcnj13*<sup>+</sup>, *Met*<sup>+</sup>, *Nrp2*<sup>+</sup>, *Cd44*<sup>+</sup>); basal cells (BC, *Tjp1*<sup>high</sup>, *Cldn11*<sup>+</sup>); and MC (*Kcnq1*<sup>+</sup>, *Kcne1*<sup>+</sup>) [22–24]. UMAP showed well-separated clusters with significant enrichment of marker genes for the respective cell types in each treatment (Fig. 1A–D). Then, the four separated cochlear SVs with the same specific cells were integrated in the following analysis with the fast, sensitive and accurate integration algorithm called Harmony (Fig. 1E).

### Common conservative gene markers in IC, BC and MC of different treatments

To explore the conservative expression pattern of three major cell types in different treatments, the top 100 cluster-defining genes for each cell type ranked by avg\_log2FC with Seurat FindAllMarkers were extracted. The intersection of the top 100 genes in three major cell types of different treatments was mapped using the R package VennDiagram (1.7.3). The results showed a total of 36, 11, and 29 common conservative genes of IC, BC, and MC in the four treatments, respectively (Fig. 2A, C, E, Table 2).

These common genes enriched in KEGG pathway using clusterProfiler package are involved in a wide range of biological process mainly such as pigmentation-related pathways (pigment production, development, metabolic and biosynthetic process), cell adhesion and migration (focal adhesion and ECM-receptor interaction), ATP related pathways (positive regulation and regulation of ATP-dependent activity) and signal transduction (calcium signaling and PI3K-Akt signaling pathway) in IC; cell migration and proliferation related pathways (negative regulation of cell migration, cell mobility, locomotion, smooth muscle cell proliferation and muscle cell adaptation, regulation of smooth muscle cell proliferation and endothelial cell migration), cell signaling and survival (protein kinase pathway and MAPK signaling pathway), cell–matrix interactions (focal adhesion and ECM-receptor interaction), and ATP related pathways (ATP metabolic process and regulation of ATP-dependent activity) in BC; potassium ion transmembrane transport

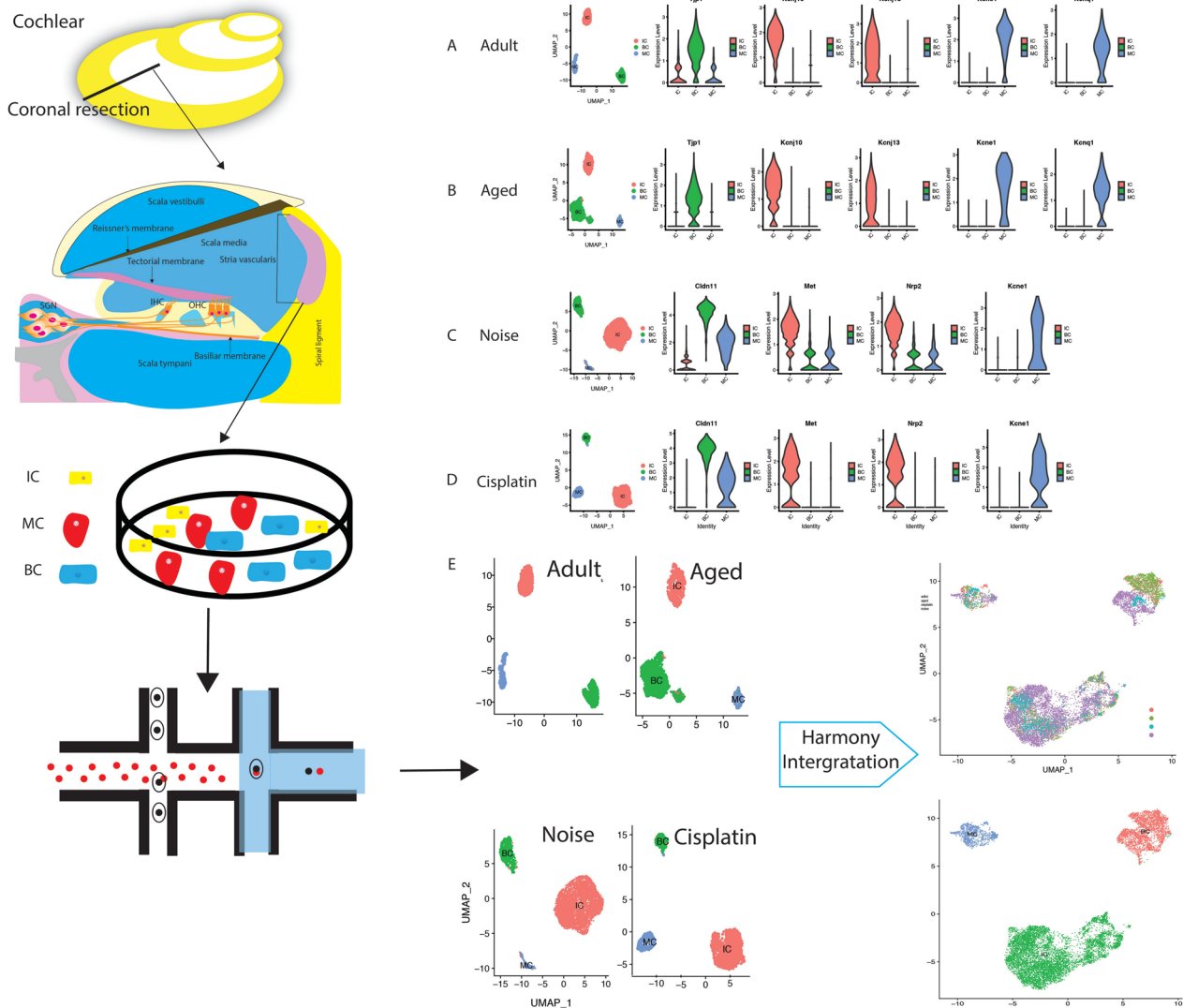


**Fig. 1** Integrative online published single-cell transcriptomic sequencing (scRNA-seq) datasets of mouse cochlear stria vascularis (SV) from sensorineural hearing loss (SNHL). Uniform manifold approximation and projection (UMAP) plot of the identified cell populations and violin plot of the expression of known marker genes in the identified cell populations of SV from adult (A), age-related hearing loss (ARHL) (B), noise-related hearing loss (NRHL) (C) and cisplatin-related hearing loss (CRHL) (D) mouse cochlea. E Schematic flowchart showing the integration and generation of an integrated dataset from online published scRNA-seq datasets of mouse cochlea SV from different treatments (CRA004814, GSE165662, and GSE168041). IC, intermediate cells; BC, basal cells; MC, marginal cells

related pathways (regulation and negative regulation of potassium ion transmembrane transport), sodium ion transmembrane transport related pathways (positive regulation of sodium ion transmembrane transport, cellular sodium ion homeostasis), cell–matrix interactions (focal adhesion and ECM-receptor interaction), ATP related pathways (regulation of ATP metabolic process and ATP-dependent activity, positive regulation of ATP-dependent activity) and cell signaling and survival (extrinsic apoptotic signaling pathway, protein

kinase B signaling and MAPK signaling pathway) in MC (Fig. 2B, D, F).

### Similar and different signaling pathways within SNHL

To investigate the differences in cell populations and their corresponding molecular transcriptional characteristics, we compared SV samples from the aged group and those exposed to noise and cisplatin with adult SV samples, following the removal of batch effects.

As in the dataset, adult and other treated SV cells were integrated using an anchor-based integration method.

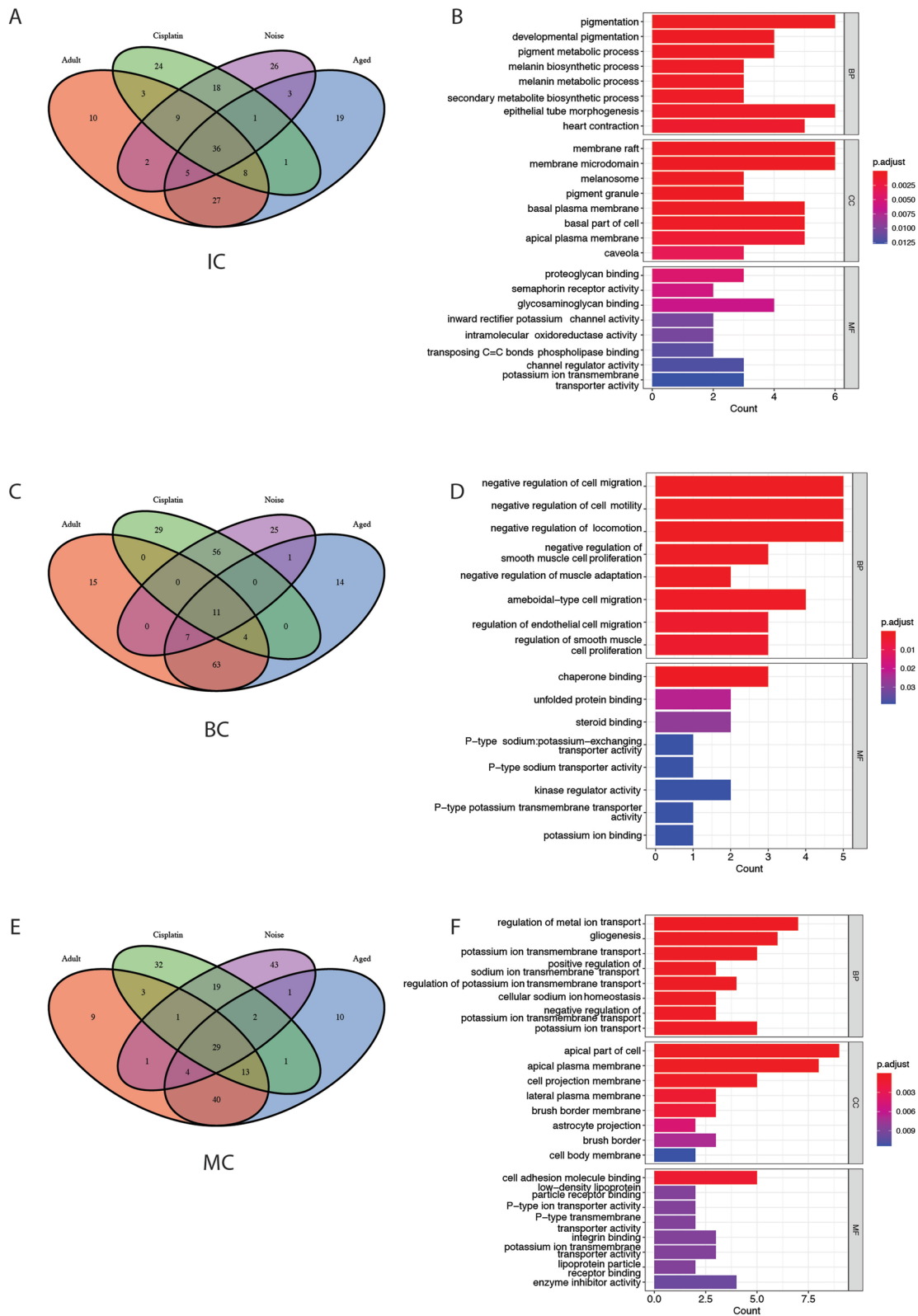


**Fig. 2** Novel gene markers of cochlear SV subtype cells and their pathway clustering. Common conserved genes among the SV major cells: IC (A), BC (C) and MC (E) with different treatments. Kyoto Encyclopedia of Genes and Genomes (KEGG) pathway enrichment analysis of common conserved genes in IC (B), BC (D) and MC (F). IC, intermediate cells; BC, basal cells; MC, marginal cells, SV, stria vascularis

**Table 2** List of common conserved genes in SV subtypes

IC	BC	MC
Dct, Gsta4, Atp1b1, Gpnmb, Ifi2712a, Hpse, Mlna, Tyr, Fxyd3, Slc45a2, Ednrb, Dlc1, Met, Kcnj10, Kcnj13, Syng1, Oxct1, Taf1d, Syt4, Tbx2, Nrip2, Edil3, Rapgef4, Scn1b, Dkk3, Scrg1, Ctsb, 5031439G07Rik, Plp1, Phlda1, Pax3, Ncam1, Cox8b, Mpz1, Cd44, Adm	Apod, Cp, Igfbp5, Ebf1, Hsbp1, Clu, Ifitm1, Fn1, Atp1a2, Nr2f2, Klf4	Dhase1, Spp1, Lrp2, Gas2, Dc1k1, Kcne1, Lrpap1, Ank3, Mt3, Atp1b2, Igf1, Rspo3, Hspa4l, Gpx3, Enpep, Epcam, Reep5, Itgb5, Tesc, Rgs4, Padi2, Spint2, Wfdc2, Mal, Mtch1, Atp2b1, Tnfrsf21, Kcnk1, Ktt18

Well-separated clusters in the UMAP plot showed significant enrichment of marker genes for the respective cell types (Fig. 1E).

To detect SV cell transcriptional effects of elderly, cisplatin-treated, and noise-treated groups, we used FindMarkers with a default log<sub>2</sub>FC threshold of 0.25 to identify DEGs comparing different groups with the adult group. We compared the DEGs and created volcano plots for the distinct treatments of IC, BC, and MC. We observed that the three subsets of cells showed a higher similarity in DEGs between the cisplatin and noise treatment groups (Fig. 3A, C, E). We found 698 upregulated and 505 downregulated genes in the elderly group, 1457 upregulated and 2305 downregulated genes in the cisplatin-treated group, and 1640 upregulated and 2449 downregulated genes in the noise-treated group. The list of differentially expressed genes obtained from the differential analysis can be found in Supplementary Table S1 for specific details. We then filtered these differentially expressed genes with an absolute log<sub>2</sub>FC greater than or equal to 0.6 and performed GSEA enrichment on these DEGs, setting the FDR to less than or equal to 0.05. We found that different treatment groups had similar downregulated enrichment pathways in oxidative phosphorylation and electron transport chain (Fig. 3B, D, F, Supplementary Table S2). Oxidative phosphorylation and electron transport chain are both mitochondrial energy metabolism pathways involved in cellular ATP synthesis. The results suggest that these pathways are suppressed in aged, cisplatin-treated, and noise-treated cells, indicating a common impact on cellular ATP synthesis across different treatment conditions (Fig. 3G).

#### Identification of cell type-specific regulatory factors in cochlear SV specific cells and their role in mitochondrial energy metabolism

To investigate the potential molecular mechanisms driving the common gene expression of the different clusters, we used pySCENIC to comprehensively reconstruct the gene regulatory networks for three major cell types of SV (Fig. 4A). To identify cell type-specific regulatory factors in cochlear vasculature cells, we constructed gene regulatory networks in three known subtypes of cochlear

vasculature cells (IC, BC, and MC) and calculated the Regulon Specificity Scores (RSS) of candidate factors. We found that 28 regulatory factors were highly expressed in a subtype-specific manner. Using single-cell data, we confirmed the expression of these factors in the three subtypes and identified Etv1, Sox10, and Mitf as the most specific regulons associated with IC cells, Esrrb with MC cells, and Tbx18 with BC cells (Fig. 4B, D). We confirmed these cell-specific regulons using the gEAR database again (Fig. 4C).

In addition, the RSS are used to evaluate regulons and rank them in each treatment. We found that the transcriptomic factors vary in different states. The expression trends of regulatory factors in the adult and aged groups were similar, with most of them showing an upregulation trend. In contrast, the expression trends of regulatory factors in the noise and cisplatin groups were similar, with most of them showing a downregulation trend. (Fig. S4). We then investigated whether these factors were involved in previous mitochondrial energy metabolism pathways by analyzing their expression in SV cells from different treatment groups using a heatmap and ChEA Transcription Factor Targets Dataset. Our findings suggest that the regulatory factors E2f1, Esrrb, Runx1, Yy1, Nfe2l2, and Gata2 have a strong relationship with the genes of mitochondrial energy metabolism pathways (Fig. 4E).

#### Intercellular communication network inference in SNHL

Generally, SV cells should not work in isolation but instead should collaborate and establish connections by interacting with signals from their environment. To create a network of cell–cell communication within the cochlear SV, a recently developed mathematical modeling approach known as CellChat is utilized. CellChat quantitatively infers intercellular communication networks through mass action models and facilitates the visualization of cellular interactions [21].

Counting the interactions (depicted as “line” connections) among the major cochlear SV cell types using a circular plot, we constructed a comprehensive cell–cell communication network based on the ligand–receptor pairs under four distinct conditions (Fig. 5A). The

(See figure on next page.)

**Fig. 3** Volcano plot of differentially expressed genes (DEGs) in the SV subtype cells from mice with sensorineural hearing loss and bar chart of gene set enrichment analysis (GSEA) of these DEGs. DEG analysis of IC (A), BC (C) and MC (E) from age-related hearing loss (ARHL), noise-related hearing loss (NRHL), and cisplatin-related hearing loss (CRHL) datasets compared with the adult dataset are shown in volcano plot. The top ten genes in the volcano plot have been labeled, with log<sub>2</sub>FC cutoff set at 0.5 and p-value cutoff set at 0.001. DEGs in SV cells from the ARHL (B), NRHL (D), and CRHL (F) datasets compared with the adult dataset are clustered using GSEA on WebGestalt 2019. These genes clustered in the oxidative phosphorylation and electron transport chain pathways with GSEA analysis are colored in the electron transport chain from the Kyoto Encyclopedia of Genes and Genomes (KEGG) database (G). IC, intermediate cells; BC, basal cells; MC, marginal cells, SV, stria vascularis





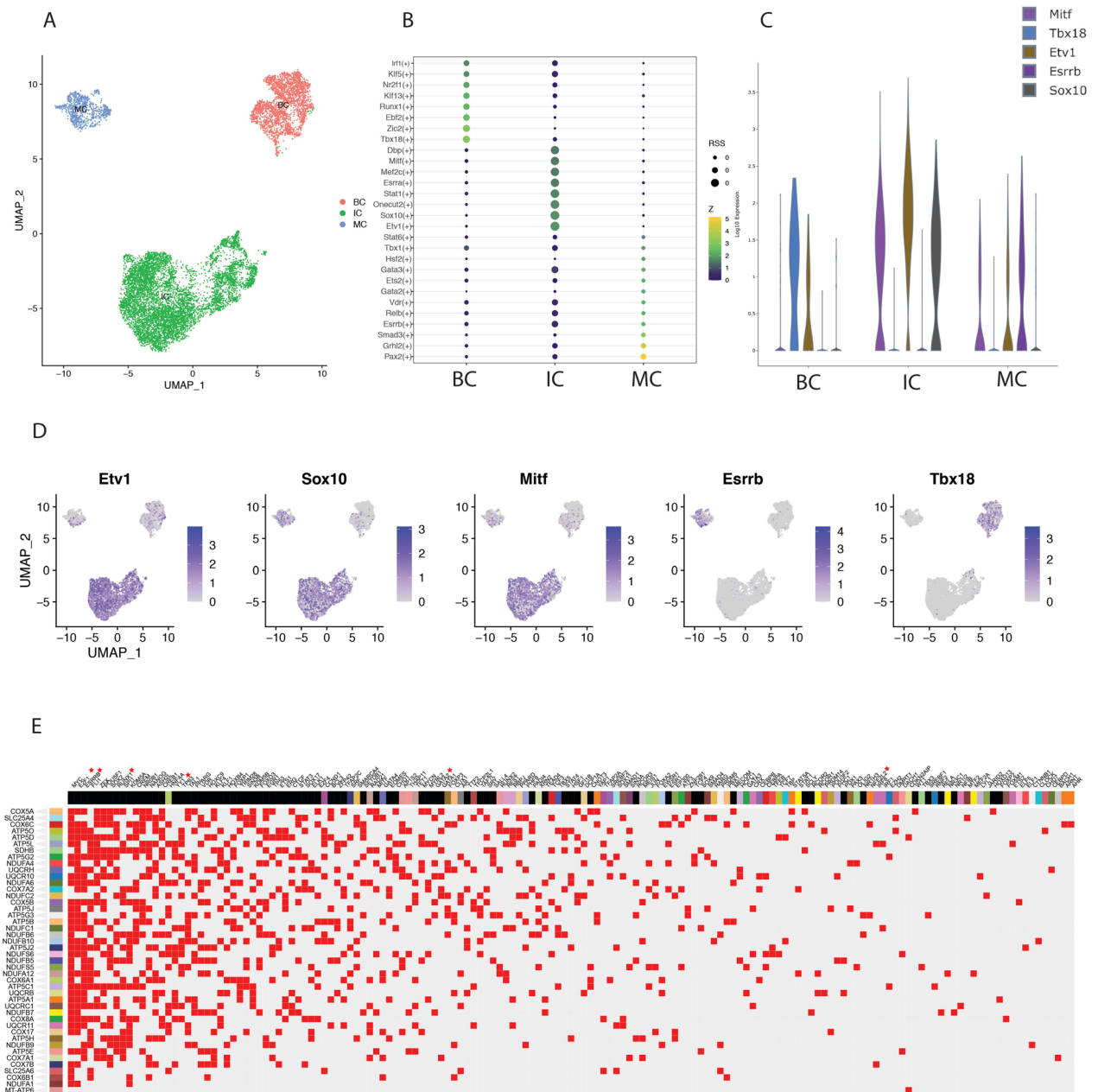
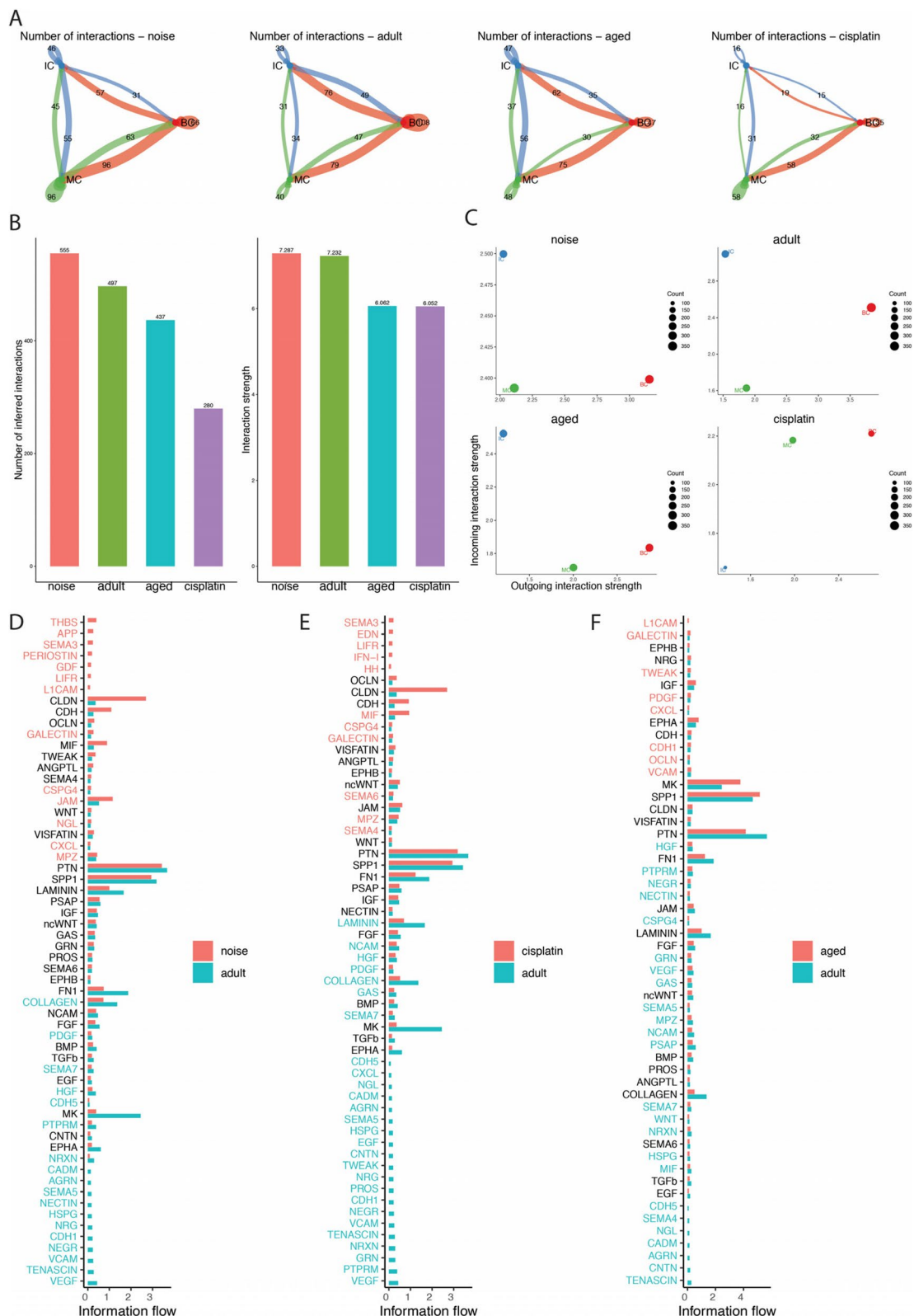


**Fig. 4** Identification of cell type-specific regulons by SCENIC analysis and prediction of target transcription factors (TF) within downstream genes (colored in Fig. 3G) using the CHEA Transcription Factor Targets Dataset in Harmonizome 3.0. Integration of the four datasets is processed and clustered into three cell-specific types (A). TFs specific to SV single-cell subpopulation are selected with calcRSS function in SCENIC (B). The representative TFs of the SV single-cell subpopulation are confirmed in the gEAR database (C) and integrated datasets (D). These genes (vertical level) clustered in the oxidative phosphorylation and electron transport chain pathways are predicted to be regulated by these TFs (horizontal level) using the CHEA Transcription Factor Targets Dataset (E). These TFs with red stars are also found in our SCENIC analysis results (Additional file 5: Fig. S5)

(See figure on next page.)

**Fig. 5** Inference of cell–cell communications by CellChat shows global alterations in signaling pathway-mediated communications between SV-specific cells in SNHL. Circle plots of the interaction numbers and interaction strength between SV-specific cells (A). The arrows indicate the direction of intercellular communication. Comparison of the total number of cell communication interactions and the strength of these interactions in bar chart (B). Changes in incoming and outgoing signaling in SV-specific cells across different datasets (C). Global comparison of the information flow of signaling pathways in SV cells between the SNHL and adult mouse groups (D, E, F)



quantities and intensities of those interactions within each SV cell group were summarized (Fig. 5C); the counts of cell–cell interactions were decreased in the cisplatin-treated and aged groups (280 and 437, respectively) compared to the adult groups (497). This reduction aligns with the decrease in the strengths of those interactions observed in the cisplatin-treated and aged groups. This decrease could be attributed to a reduction in the expression of ligands and receptors, either in the IC, BC or both (Fig. 5B). The counts of cell–cell interactions showed an increase in the noise-treated group (555) compared to the adult group (497). This increase aligns with the observed increase in the strength of these interactions in the noise-treated group. This enhancement could be attributed to an upregulation in the expression of both receivers and senders in MC (Fig. 5B).

In comparison to the adult group, the noise-treated group exhibited activation of signaling pathways such as THBS, APP, SEMA3, and several others, while pathways including VCAM, TENASCIN, VEGF and others were deactivated. Meanwhile, some pathways, such as PDGF, SEMA7, HGF, CDH5, PTPRM and NRXN, were decreased, whereas others, such as GALECTIN, CSPG4, JAM, NGL, CXCL and MPZ, were increased in the noise-treated group (Fig. 5D).

Furthermore, when compared with the adult group, the SEMA3, EDN, LIFR, IFN-1 and HH signaling pathways were turned on, whereas VEGF, PTPRM, GRN and some other signaling pathways were turned off in the cisplatin-treated group. The cisplatin-treated group showed an increase in the SEMA4, SEMA6, MIF, CSPG4, and MPZ pathways. Meanwhile, they exhibited a decrease in the LAMININ, NCAM, HGF, PDGF, GAS, COLLAGEN and SEMA7 pathways (Fig. 5E).

In comparison with the adult group, the L1CAM signaling pathway is turned on, whereas the CDH5, SEMA4, NGL, CADM, AGRN, CNTN, and TENASCIN signaling pathways are turned off in the aged group. The aged group showed an increase in the GALECTIN, TWEAK, PDGF, CXCL, CDH1, OCLN, and VCAM pathways, while it exhibited a decrease in HGF, PTPRM, NEGR and some other signaling pathways compared with the adult group (Fig. 5F).

At the same time, the findings obtained from CellChat indicated that IC displayed reduced incoming

interaction strength (the communication probabilities of the incoming signaling to a cell population) in the treated groups compared to the adult group (Fig. S2). As a result, we conducted further investigation into the signaling pathways through which ICs function as receivers and BCs and MCs act as senders in subsequent analyses. By taking the intersections, we found that the significantly increased signaling pathways common to all three treated groups, compared with the adult group, were GALECTIN (Lgals9–Cd44), mainly concentrated in IC cell autocrine signaling (Fig. 6). The significantly decreased common signaling pathways were PTPRM (Ptpm–Ptpm), NRXN (Nrxn1–Nlgn1), and COLLAGEN (Col1a2–Sdc4, Col1a2–Cd44) (Fig. 6). Combining the CHEA Transcription Factor Targets Dataset and our data, we found that the transcription factor Nfe2l2 is related to these common signaling pathways and varies in different treatment groups.

## Discussion

Comprehending the molecular response of the inner ear to both external and internal causative factors that induce damage is essential for the strategic development of targeted therapeutics to address sensorineural hearing loss (SNHL), including NIHL, ARHL and CRHL. Research indicates that proper functioning of the SV is crucial for the survival of adult outer hair cells (OHCs). Interestingly, the survival and normal function of the SV appear to be independent of the functionality of hair cells [25]. In this context, we offer a thorough analysis of the transcriptomes specific to SV cell types within the adult mouse cochlea, considering the effects of aging, cisplatin exposure, and noise exposure.

We utilized known SV major cell-type-specific markers to extract IC, BC, and MC from the data of each treatment group separately. Through analysis, we discovered that different treatment groups exhibit similar conserved genes in various subtypes of cells. We intersected the top 100 highly expressed genes from each treatment group in the same subtype cells (Additional file 1, 2 and 3: Fig. S1-3A) and these common genes are also supported by the gEAR database (Additional file 1, 2 and 3: Fig. S1-3B) [26]. Novel marker genes that exhibit specific expression in IC include *Atp1b1*, *Dct*, and *Adm*. *Atp1b1* and *Dct* were found to be downregulated in the whole cochlea of

(See figure on next page.)

**Fig. 6** Cell–cell signaling interactions between each cell cluster in SV with different treatments. Highlighted significant interactions in SV-specific cells between the NRHL and adult groups (A, B). Highlighted significant interactions in SV-specific cells between the CRHL and adult groups (C, D). Highlighted significant interactions in SV-specific cells between the ARHL and adult groups (E, F). Dot color reflects communication probabilities, and dot size represents computed p values computed from a one-sided permutation test. Empty space means that the communication probability is zero

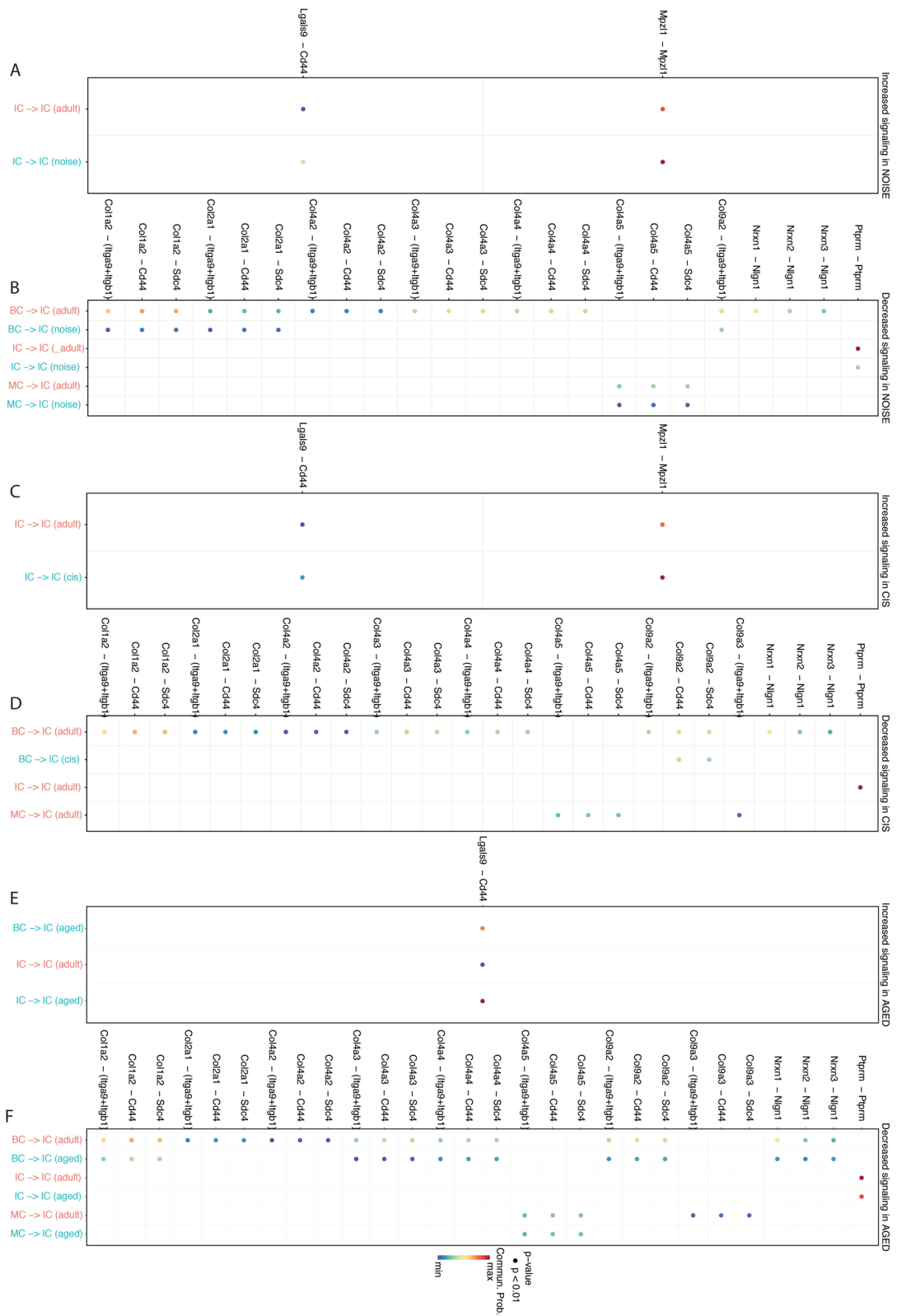


Fig. 6 (See legend on previous page.)

aging mice [24], but we observed their relative conservation in the SV across all treatment groups. The expression of *Dct* is higher in the control group compared with postnatal 3-day *Tbx1* mutation mice in IC of the SV [27]. Additionally, *Dct* showed significantly higher expression in IC of the noise-exposed treatment group compared with other groups. BC showed specific significant expression of new marker genes such as *Apod*, *Clu*, and *Igfbp5*. *Clu* expression in BC was reported by Lee [28]. Zhao et al. found that adult *Clu*-null mice displayed fewer hair cells and hearing loss [29]. Garcia-Mato A et al. found *Igfbp5* expressed in hair cells, Deiters' cells and pillar cells in the adult mouse cochlea [30]. *Apod* could be detected in the spiral ligament, spiral limbus and OHC in 3-week mice [31]. MC cells exhibited specific significant expression of new marker genes, including *Lrp2*, *Gas2*, *Dclk1*, *Igf1*, *Itgb5*, *Tesc*, *Rgs4*, and *Padi2*. *Lrp2*, *Igf1*, and *Dclk1* were downregulated in the whole cochlea of aging mice [24], which is consistent with the findings of He et al. [32] that *Igf1* is downregulated in aging mouse hair cells. *Lrp2* is expressed enormously in the MC in mouse cochlea and this was identified by smFISH, single-cell and single-nucleus RNAseq in 2023 [33]. *Padi2* and *Gas2* were found to be downregulated in the vasculature of cisplatin-treated mice [23]. Chen T et al. found *GAS2* mutations resulted in disorganization and destabilization of microtubule bundles in humans and mice inner ear supporting cells [34]. *Rgs4* immunofluorescence could be detected in the auditory nerve fibres and SV in 6–8 weeks rat [35]. *Adm* is a potential novel marker gene for IC, while *Itgb5* and *Tesc* are potential novel marker genes for MC in the cochlea. These speculations still require further immunohistochemical validation in the inner ear.

In addition, we merged the same subtype cells from four different treatment groups, and through pySCENIC analysis, we identified transcription factors with specific high expression in IC, BC, and MC (Fig. 4B). Analysis using the CHEA Transcription Factor Targets Dataset revealed that the conserved genes *Dct*, *Cd44*, *Adm*, *Tbx2*, *Syng1*, *Dlc1*, *Ctsb*, *Ednrb*, *Kcnj10*, *Mlana*, *Oxct1*, *Pax3*, *Phlda1*, *Plp1*, *Slc45a2*, *Met*, *Tyr*, and *Nrp2* are downstream targets of the specific transcription factor *Mitf* in IC. The conserved gene *Clu* is a downstream target of the specific transcription factor *Runx1* in BC. The conserved genes *Spint2*, *Kcnk1* and *Epcam* are downstream targets of the specific transcription factor *Gata3* in MC. Through KEGG analysis, we found that these conserved genes in IC are mainly associated with cytoskeleton-related pathways, while these conserved genes in BC are primarily linked to cell migration and proliferation-related pathways. These conserved genes in MC are mainly associated with potassium ion transmembrane transport-related pathways. Consequently, the impact of cisplatin,

noise exposure, and aging factors on these genes and their associated pathways within the SV appears to be relatively limited.

Research on bulk data and single-cell transcriptomics related to sensory neural hearing loss currently mainly focuses on inner ear hair cells. Studies have found that major causal factors inducing sensory neural hearing loss, such as aging, noise, and drug-related factors, share common pathways for damage to inner ear hair cells: apoptosis, the immune response, and inflammation [19]. The changes observed in OHCs during aging and in response to noise exposure involve common processes, including the immune response, cellular response to stress, regulation of transmembrane transport, and ion channel regulation. However, there is not much single-cell transcriptomic research available concerning vascular lesions in sensory neural hearing loss. Milon et al. showed that SV epithelial cells, including MCs, ICs and BCs, exhibited a shared upregulated response enriched in innate immune functions and downregulated response observed in genes related to potassium ion transport following exposure to noise [22]. Decreases in genes related to endocochlear potential (*Kcne1*, *Kcnq1*, *Atp1b2*, *Slc12a2*, *Met*, *Gjb2*) were observed in the transcriptional response of SV cell subtypes to cisplatin [23].

In our study, we compared the transcriptome genes of three major SV cell types from the aging, cisplatin exposure, and noise exposure groups with the adult group. We observed a significant overlap in DEGs between the noise and cisplatin exposure groups (Fig. 3A, C, E). Subsequently, we conducted GSEA separately for these differentially expressed genes and identified a common downregulation of the signaling pathways related to oxidative phosphorylation and electron transport chain in all three treatment groups. Both of these pathways are involved in mitochondrial energy metabolism and play a crucial role in cellular ATP synthesis (Fig. 3B, D, F). We also marked the positions of these cluster genes within the electron transport chain, and these genes are involved in nearly all processes of the electron transport chain. Through pySCENIC, we conducted an analysis of transcription factor differences among the three main cell types in SV under different treatments. There were varying levels of transcription factor expression changes among the groups (Additional file 5: Fig. S5). Using CHEA Transcription Factor Targets Dataset analysis, we identified important transcription factors corresponding to genes in the electron transport chain, including *E2f1*, *Esrrb*, *Runx1*, *Yy1*, *Nfe2l2*, and *Gata2*. These transcription factors may be crucial common targets regulating sensorineural hearing loss caused by different treatments (Fig. 4E). Gomez-Dorado M et al. found that *E2F1* could regulate the mammalian *ATOH1* and implied

its potential of hair cell regeneration in the inner ear [36]. ESRRB mutations are identified to result in congenital hearing impairment in human [37]. Runx1 is found necessary for generation of SGN subtype identities and controls auditory sensory neuron diversity in mice [38]. Nfe2l2 has been linked to SNHL and is observed in the cochlear SV. However, its distribution in the cochlea differs between humans and animals [39]. Gata2 deficiency is associated with syndromic hearing loss [40]. Except for Nfe2l2, none of these transcription factors have been reported in the cochlear SV.

SNHL is also associated with inflammation factors [41]. We selected classic inflammatory factors interleukin (IL)-6, tumor necrosis factor- $\alpha$  (TNF- $\alpha$ ), and nuclear factor kappa B (NF- $\kappa$ B) related to SNHL. We compiled the average log<sub>2</sub>FC of these relevant inflammatory factors in the Supplementary Table S3. Some classic inflammatory factors were not included in DEGs and were instead clustered in GSEA. That may result from the beginning setting of the absolute value of log<sub>2</sub>FC greater than or equal to 0.6 when filtering differentially expressed genes. Consequently, some factors in the inflammatory pathways might have been filtered out, which could be a reason for the lack of enrichment of inflammatory pathways. These classic inflammatory factors show consistent elevation in ARHL. However, they exhibit inconsistent trends in NRHL and CRHL. This discrepancy might also be one of the reasons why the inflammatory factors failed to be enriched.

Current research on single-cell interactions between SV-subspecific cells in NRHL is limited [22]. We conducted integrated data analysis to examine the detailed changes in cell communication among different subtypes of SV in the cochlea following various treatments. Our findings indicate that, compared with adult mouse cochlear SV, there is an increased interaction between the three main subtypes of SV after noise exposure, particularly with enhanced incoming and outgoing interaction strength in the MC and increased outgoing interaction strength in the IC. This suggests that following acute injury from noise exposure, the MC in the SV attempts compensatory mechanisms to restore the physiological state of the cochlear supporting cells, particularly endolymphatic potential (EP) maintenance. Furthermore, our previous results revealed a higher expression of conservative potassium ion transmembrane transport pathway genes in MC, which may be related to these observed changes. Globally, there is a decrease in the number of interactions among various SV cell types, a trend that aligns with the decrease in interaction strength observed in both CRHL and ARHL. Our findings indicated that there is a reduction in incoming and outgoing interaction strength

primarily in BC of the ARHL and in IC and BC of the CRHL. This indicates that the disruption of cellular pathway regulation induced by acute cisplatin injury in the SV primarily occurs in the IC and BC. Sluyter et al. [7], through electron microscopy studies, found that SV leads to significant thinning of the IC layer in the cochlear basal turn after low-dose chronic cisplatin injury, but there are no significant changes during the acute phase. During the recovery period after acute cisplatin injury, the BC layer undergoes significant thinning. Therefore, we speculated that although there are no significant morphological changes during the acute cisplatin injury phase in the SV, alterations in the communication pathways between cells are the reason for the disruption of high-concentration potassium ion secretion, leading to a reduction in EP. Our findings also indicate that the disruption of cellular pathway regulation induced by aging degeneration in the SV primarily occurs in BC. Cdh1, Col1a2, Col2a1, Col4a2, Col4a3, Col4a4, Col9a2, Nrnx1, Nrnx2 and Vegfb-related signaling pathways are decreased in BC (Fig. 6F). Mutations in Col1a2 are associated with osteogenesis imperfecta, while mutations in Col2a1 and Col9a2 are linked to Stickler syndrome [42]. Both conditions are characterized by progressive hearing loss. Col4a2, Col4a3, and Col4a4 are associated with Alport's syndrome, a condition characterized by progressive hearing loss [43].

After exploring the global common molecular mechanisms in cochlear SV following different treatments, we further investigated alterations in the molecular pathways between three major cells of the SV to identify more precise and specific coregulatory pathways. A similar downregulation trend in the incoming interaction strength of IC across the three types of SNHL was observed (Additional file 4: Fig. S4). Consequently, we focused our attention on the incoming interaction pathways in IC. We found an upregulation trend in the IC incoming signaling pathway of GALECTIN: Lgals9–Cd44 among the three types of SNHL. This signaling pathway is characterized by autocrine behavior of IC. Furthermore, we discovered that the pathways involving PTPRM: Ptpm–Ptpm, NRXN: Nrnx1–Nlgn1, and COLLAGEN: Col1a2–Sdc4/Cd44 exhibited similar downregulation trends in IC, with signals primarily originating from autocrine and paracrine secretion of BC across all three types of SNHL (Fig. 6). Galectin-9-Cd44 interaction could enhance stability and function of adaptive regulatory T cells in mice [44]. It had showed that Nlgn1 knockout mice cochleae had fewer ribbon synapses resulting in impaired hearing [45]. Lgals9–Cd44, Ptpm–Ptpm, Nrnx1–Nlgn1, and Col1a2–Sdc4/Cd44 may represent novel regulatory pathways in cochlear SV pathology associated with SNHL.

We found that Nfe2l2 target genes prediction included Ptpm, Nrnx1 and Col1a2 using CHEA Transcription Factor Targets Dataset. Combining our previous analysis of transcriptional regulators in the regulation of the electron transport chain, we predicted that the TF Nfe2l2 might act as a key regulator of Ptpm, Nrnx1, Col1a2 and electron transport chain. Nfe2l2 is downregulated in IC from CRHL and NRHL (Additional file 6: Fig. S6). Our previous research has shown that the antioxidant astaxanthin can protect mitochondrial membrane potential and mitigate cisplatin-induced apoptosis of cochlear outer hair cells through the regulation of the Nfe2l2 pathway [46]. Honkura et al. found that increasing Nfe2l2 and its downstream gene expression levels were beneficial in preventing noise-induced hearing loss [47]. Oishi et al. discovered that activation of the Nfe2l2 pathway in the mouse cochlea could prevent ARHL through alleviating oxidative stress-induced damage caused [48]. Hence, our hypothesis posits that the regulation of Nfe2l2 may have a modulatory effect on Ptpm, Nrnx1, Col1a2, and electron transport chain, rendering Nfe2l2, Ptpm, Nrnx1, and Col1a2 potential targets for drug intervention in the treatment of SNHL.

## Conclusion

Our bioinformatics analysis has revealed that despite differences in the pathogenesis of ARHL, CRHL and NRHL, they share common pathways in cochlear SV: oxidative phosphorylation and the electron transport chain, both of which are associated with mitochondrial energy metabolism. Downregulation of the mitochondrial electron transport chain has been observed in various conditions of SNHL. E2f1, Esrrb, Runx1, Yy1, and Gata2 could serve as novel important common TFs regulating the electron transport chain. Adm has emerged as a potential new marker gene for IC, while Itgb5 and Tesc show promise as potential new marker genes for MC in the SV. Our research has discovered signaling disruptions among SV cells in sensorineural hearing loss, with specific cells exhibiting distinct trends and similar trends under varying treatment conditions. These findings offer a new perspective on SV lesions in SNHL and provide additional theoretical evidence for the same drug treatment and prevention of different pathologies of SNHL.

## Supplementary Information

The online version contains supplementary material available at <https://doi.org/10.1186/s12864-024-10122-7>.

Supplementary Material 1.  
Supplementary Material 2.  
Supplementary Material 3.  
Supplementary Material 4.

Supplementary Material 5.  
Supplementary Material 6.  
Supplementary Material 7.  
Supplementary Material 8.  
Supplementary Material 9.

## Acknowledgements

The authors appreciate Dr. Jimmy Zeng (University of Macau) for his experience with data analysis.

## Authors' contributions

BYN, XSH, and XG conceptualized and designed the study. RRC, KLJ, and ZFC conducted the integration of the three publicly available scRNA-seq datasets of the mouse cochlear SV, followed by further data processing and analysis of the integrated scRNA-seq dataset. XMW analyzed and interpreted the data and authored the manuscript. BYN and XG contributed to manuscript writing and revision. HJX provided assistance in data analysis. All authors reached a consensus and gave their approval for the final manuscript.

## Funding

This research received financial support from the following sources: the National Natural Science Foundation of China (Grant No. 82201272), the Natural Science Foundation of Fujian Province (Grant No. 2022J01217), the Young and Middle-aged Key Personnel Training Project of Fujian Provincial Health Commission (Grant No. 2021GGA024), and the Medical Science and Technology Project of Zhejiang Province (Grant No. 2023RC047).

## Availability of data and materials

This study involved the analysis of publicly available datasets, which can be accessed through the following links: <https://www.ncbi.nlm.nih.gov/geo/query/acc.cgi?acc=GSE165662>, <https://www.ncbi.nlm.nih.gov/geo/query/acc.cgi?acc=GSE168041>, and <https://ngdc.cnc.ac.cn/bioproject/browse/PRJCA006213>.

## Declarations

### Ethics approval and consent to participate

This article does not contain any studies with human participants or animals.

### Consent for publication

Not applicable.

### Competing interests

The authors declare no competing interests.

### Author details

<sup>1</sup>Department of Otorhinolaryngology, the Second Affiliated Hospital and Yuying Children's Hospital of Wenzhou Medical University, Wenzhou, China. <sup>2</sup>Department of Otorhinolaryngology, Head and Neck Surgery, the First Affiliated Hospital, Fujian Medical University, Fuzhou, China. <sup>3</sup>Fujian Institute of Otolaryngology, the First Affiliated Hospital, Fujian Medical University, Fuzhou, China. <sup>4</sup>Department of Otorhinolaryngology, Head and Neck Surgery, National Regional Medical Center, Binhai Campus of the First Affiliated Hospital, Fujian Medical University, Fuzhou, China. <sup>5</sup>Department of Otorhinolaryngology-Head and Neck Surgery, Zhongshan Hospital, Fudan University, Fenglin Road 180, Xuhui District, Shanghai 200030, People's Republic of China. <sup>6</sup>Department of Otolaryngology-Head and Neck Surgery, the First Affiliated Hospital of Wenzhou Medical University, Wenzhou, China.

Received: 14 November 2023 Accepted: 14 February 2024  
Published online: 27 February 2024

## References

- Hudspeth AJ. SnapShot: auditory transduction. *Neuron*. 2013;80(2):536 e531.



2. Cunningham CL, Müller U. Molecular Structure of the Hair Cell Mechano-electrical Transduction Complex. *Cold Spring Harb Perspect Med.* 2019;9(5):a033167.
3. Wangemann P. Supporting sensory transduction: cochlear fluid homeostasis and the endocochlear potential. *J Physiol.* 2006;576(Pt 1):11–21.
4. Zdebik AA, Wangemann P, Jentsch TJ. Potassium ion movement in the inner ear: insights from genetic disease and mouse models. *Physiology (Bethesda).* 2009;24:307–16.
5. Basch ML. Building a sound wall in the cochlea: development of the stria vascularis. *FASEB J.* 2019;33(S1):81.82–81.82.
6. Bartels S, Ito S, Trune DR, et al. Noise-induced hearing loss: the effect of melanin in the stria vascularis. *Hear Res.* 2001;154(1–2):116–23.
7. Sluyter S, Klis SF, de Groot JC, et al. Alterations in the stria vascularis in relation to cisplatin ototoxicity and recovery. *Hear Res.* 2003;185(1–2):49–56.
8. Breglio AM, Rusheen AE, Shide ED, et al. Cisplatin is retained in the cochlea indefinitely following chemotherapy. *Nat Commun.* 2017;8(1):1654.
9. Meech RP, Campbell KC, Hughes LP, et al. A semiquantitative analysis of the effects of cisplatin on the rat stria vascularis. *Hear Res.* 1998;124(1–2):44–59.
10. Le TN, Straatman LV, Lea J, et al. Current insights in noise-induced hearing loss: a literature review of the underlying mechanism, pathophysiology, asymmetry, and management options. *J Otolaryngol Head Neck Surg.* 2017;46(1):41.
11. Goldwyn BG, Quirk WS. Calcium channel blockade reduces noise-induced vascular permeability in cochlear stria vascularis. *Laryngoscope.* 1997;107(8):1112–6.
12. Suzuki M, Yamasoba T, Ishibashi T, et al. Effect of noise exposure on blood-labyrinth barrier in guinea pigs. *Hear Res.* 2002;164(1–2):12–8.
13. Shin SA, Lyu AR, Jeong SH, et al. Acoustic trauma modulates cochlear blood flow and vasoactive factors in a rodent model of noise-induced hearing loss. *Int J Mol Sci.* 2019;20(21):5316.
14. Shi X, Nuttall AL. Upregulated iNOS and oxidative damage to the cochlear stria vascularis due to noise stress. *Brain Res.* 2003;967(1–2):1–10.
15. Collins JG. Prevalence of selected chronic conditions: United States, 1990–1992. *Vital Health Stat 10.* 1997;(194):1–89.
16. Martinez AD, Acuna R, Figueroa V, et al. Gap-junction channels dysfunction in deafness and hearing loss. *Antioxid Redox Signal.* 2009;11(2):309–22.
17. Wang J, Puel JL. Toward cochlear therapies. *Physiol Rev.* 2018;98(4):2477–522.
18. Zhong Y, Hu YJ, Yang Y, et al. Contribution of common deletion to total deletion burden in mitochondrial DNA from inner ear of d-galactose-induced aging rats. *Mutat Res.* 2011;712(1–2):11–9.
19. Chen P, Hao JJ, Li MW, et al. Integrative functional transcriptomic analyses implicate shared molecular circuits in sensorineural hearing loss. *Front Cell Neurosci.* 2022;16:857344.
20. McInnes L, Healy J, Melville J. Umap: Uniform manifold approximation and projection for dimension reduction. *arXiv preprint arXiv:180203426* 2018.
21. Jin S, Guerrero-Juarez CF, Zhang L, et al. Inference and analysis of cell-cell communication using Cell Chat. *Nat Commun.* 2021;12(1):1088.
22. Milon B, Shulman ED, So KS, et al. A cell-type-specific atlas of the inner ear transcriptional response to acoustic trauma. *Cell Rep.* 2021;36(13):109758.
23. Taukulis IA, Olszewski RT, Korrapati S, et al. Single-Cell RNA-Seq of cisplatin-treated adult stria vascularis identifies cell type-specific regulatory networks and novel therapeutic gene targets. *Front Mol Neurosci.* 2021;14:718241.
24. Sun G, Zheng Y, Fu X, et al. Single-cell transcriptomic atlas of mouse cochlear aging. *Protein Cell.* 2023;14(3):180–201.
25. Liu H, Li Y, Chen L, et al. Organ of corti and stria vascularis: is there an interdependence for survival? *PLoS One.* 2016;11(12):e0168953.
26. Korrapati S, Taukulis I, Olszewski R, et al. Single cell and single nucleus RNA-Seq reveal cellular heterogeneity and homeostatic regulatory networks in adult mouse stria vascularis. *Front Mol Neurosci.* 2019;12:316.
27. Tian C, Johnson KR. TBX1 is required for normal stria vascularis and semi-circular canal development. *Dev Biol.* 2020;457(1):91–103.
28. Lee S, Shin JO, Sagong B, et al. Spatiotemporal expression patterns of clusterin in the mouse inner ear. *Cell Tissue Res.* 2017;370(1):89–97.
29. Zhao X, Henderson HJ, Wang T, et al. Deletion of clusterin protects cochlear hair cells against hair cell aging and ototoxicity. *Neural Plast.* 2021;2021:9979157.
30. Garcia-Mato A, Cervantes B, Murillo-Cuesta S, et al. Insulin-like growth factor 1 signaling in mammalian hearing. *Genes (Basel).* 2021;12(10):1553.
31. Hildebrand MS, de Silva MG, Klockars T, et al. Expression of the carrier protein apolipoprotein D in the mouse inner ear. *Hear Res.* 2005;200(1–2):102–14.
32. Liu H, Giffen KP, Chen L, et al. Molecular and cytological profiling of biological aging of mouse cochlear inner and outer hair cells. *Cell Rep.* 2022;39(2):110665.
33. Faridi R, Yousaf R, Gu S, et al. Variants of LRP2, encoding a multifunctional cell-surface endocytic receptor, associated with hearing loss and retinal dystrophy. *Clin Genet.* 2023;103(6):699–703.
34. Chen T, Rohacek AM, Caporizzo M, et al. Cochlear supporting cells require GAS2 for cytoskeletal architecture and hearing. *Dev Cell.* 2021;56(10):1526–1540. e1527.
35. Fok C, Bogosanovic M, Pandya M, et al. Regulator of G protein Signalling 4 (RGS4) as a novel target for the treatment of sensorineural hearing loss. *Int J Mol Sci.* 2020;22(1):3.
36. Gomez-Dorado M, Daudet N, Gale JE, et al. Differential regulation of mammalian and avian ATOH1 by E2F1 and its implication for hair cell regeneration in the inner ear. *Sci Rep.* 2021;11(1):19368.
37. Weber ML, Hsin HY, Kalay E, et al. Role of estrogen related receptor beta (ESRRB) in DFN35B hearing impairment and dental decay. *BMC Med Genet.* 2014;15:81.
38. Shrestha BR, Wu L, Goodrich LV. Runx1 controls auditory sensory neuron diversity in mice. *Dev Cell.* 2023;58(4):306–319.e305.
39. Li D, Zhao H, Cui ZK, et al. The role of Nrf2 in Hearing Loss. *Front Pharmacol.* 2021;12:620921.
40. Homan CC, Venugopal P, Arts P, et al. GATA2 deficiency syndrome: a decade of discovery. *Hum Mutat.* 2021;42(11):1399–421.
41. Li L, Chen D, Lin X, et al. Understanding the role of inflammation in sensorineural hearing loss: current goals and future prospects. *Brain-X.* 2023;1(3):e34.
42. Bath F, Swanson D, Zavala H, et al. Hearing outcomes in stickler syndrome: variation due to COL2A1 and COL11A1. *Cleft Palate Craniofac J.* 2022;59(8):970–5.
43. Alves FR, De AQR. Revision about hearing loss in the Alport's syndrome, analyzing the clinical, genetic and bio-molecular aspects. *Braz J Otorhinolaryngol.* 2005;71(6):813–9.
44. Wu C, Thalhamer T, Franca RF, et al. Galectin-9-CD44 interaction enhances stability and function of adaptive regulatory T cells. *Immunity.* 2014;41(2):270–82.
45. Ramirez MA, Ninoyu Y, Miller C, et al. Cochlear ribbon synapse maturation requires Nlgn1 and Nlgn3. *iScience.* 2022;25(8):104803.
46. Nan B, Zhao Z, Jiang K, et al. Astaxanthin attenuates cisplatin ototoxicity in vitro and protects against cisplatin-induced hearing loss in vivo. *Acta Pharm Sin B.* 2022;12(1):167–81.
47. Honkura Y, Matsuo H, Murakami S, et al. NRF2 is a key target for prevention of noise-induced hearing loss by reducing oxidative damage of cochlea. *Sci Rep.* 2016;6:19329.
48. Oishi T, Matsumaru D, Ota N, et al. Activation of the NRF2 pathway in Keap1-knockdown mice attenuates progression of age-related hearing loss. *NPJ Aging Mech Dis.* 2020;6(1):14.

## Publisher's Note

Springer Nature remains neutral with regard to jurisdictional claims in published maps and institutional affiliations.